[CANCER RESEARCH 62, 7042–7049, December 1, 2002]

Vascular Endothelial Growth Factor Secretion by Tumor-infiltrating Macrophages Essentially Supports Tumor Angiogenesis, and IgG Immune Complexes Potentiate the Process

Emilio Barbera-Guillem,[1] Julie K. Nyhus, Chris C. Wolford, Chad R. Friece, and James W. Sampsel,

BioCrystal Ltd. Research Laboratories, Westerville, Ohio 43082-8888

ABSTRACT

Tumor growth requires neoangiogenesis. Members of the vascular endothelial growth factor (VEGF) family play an important role as angiogenic promoters in malignant tumors. Tumor cells and stromal cells are sources of VEGF in the tumor. We tested the relevance of the tumor-infiltrating macrophage (TIM) contribution as a source of VEGF in the tumor environment and the role of the local immune complexes in inducing the TIM release of VEGF. Colon and breast carcinoma biopsies were studied with immunoperoxidase staining of CD11b, sialyl-Tn (sTn) antigen (Ag), and γ immunoglobulin (IgG). The presence of TIM containing phagosomes positive for both IgG and sTn Ag was observed in all tumors, showing that TIMs endocytosed local immune complexes. Reverse transcription-PCR analysis of macrophage (MO) mRNA showed VEGF-A and -B, but not VEGF-C or -D. That pattern was not modified by the presence of tumor cells. *In vitro*, the interaction of tumor cells and MO promoted the secretion of MO VEGF. The MO secretion of VEGF was augmented when tumor cells were added to cocultures containing MOs and polymorphonuclear cells. Immune complexes formed with tumor sTn Ag and IgG induced a 5-fold increase of MO VEGF secretion. *In vivo*, TIMs and neoangiogenesis were associated. *In vivo* experiments with severe combined immunodeficient and athymic nude (*nu/nu*) mice showed increased number of TIMs, increased tumor angiogenesis, and faster tumor growth in mice with significant serum anti-sTn IgG. This study demonstrates that VEGF secreted by TIMs represents an essential support for tumor angiogenesis and growth, certainly influenced by the humoral antitumor immune response.

INTRODUCTION

Plasma concentrations of VEGF[2] are augmented in cancer patients in correlation with the extent of the disease (1–4), which suggests that the source of this factor is the tumor tissue. Furthermore, experimental tumor models produced by injecting genetically manipulated tumor cells directly into the tissues have also suggested that tumor cells are the main source of VEGF (5–7). It is a common consensus that tumor cells are capable of producing VEGF that autostimulates neoangiogenesis of neoplastic tissue and tumor growth (8). However, similar models of *in vivo* tumor growth with no genetically manipulated tumor cells have shown that if host fibroblasts do not produce VEGF, tumor growth is impaired (9), suggesting that tumor cell-derived VEGF is important but not sufficient to automaintain tumor growth. Detailed pathology studies of tumors reveal that the source of VEGF is not exclusively tumor cells; fibroblasts also show important expression of this angiogenic factor (10). In glioblastomas, normal astrocytes located outside the tumor are the most important source of VEGF (11). It was suggested that the stimulant of VEGF production in tumors should be hypoxia (12), which can be produced when there is an overwhelming growth of the tumor tissue. However, it has been observed that hypoxia is not a key stimulant of VEGF production in the tumor (13). Micrometastatic growth, for example, can be inhibited by antiangiogenic factors such as angiostatin (14), but micrometastases do not have enough mass to justify hypoxia and are normally established surrounding capillaries (15). These observations, added to progressive analysis of tumor angiogenesis, are generating questions about the actual contribution of tumor tissue cellular components to tumor behavior (16–18).

Cellular sources of VEGF, other than tumor cells, are multiple. Most of these sources are involved in normal adult tissue repair and remodeling processes. Mast cells and muscle cells are an important source of VEGF (19, 20). Fibroblasts, PMN cells, and monocytes (MOs) are sources of VEGF in the wound-healing process (21, 22). Multiple factors, including hypoxia, nitric oxide, and inflammatory cytokines such as MCP-1 (23), interleukin 1, and interleukin 6, are involved in controlling VEGF expression in normal tissue repair and remodeling events (24, 25, 26).

Angiogenesis inhibition is a target for anticancer therapy. In this scenario, the definitions of the actual cellular producers of VEGF in quantities sufficient to promote tumor growth and of the molecular mechanisms involved in stimulating those cells to produce VEGF are fundamental.

This study is an analysis of the importance of MOs infiltrating the neoplastic tissue as a source of VEGF within the tumor structure and the importance of the antitumor immune response in sustaining MO contribution to tumor neoangiogenesis.

MATERIALS AND METHODS

Mice and Cells. Normal C3H, *nu/nu* beige mice, and SCID beige mice were purchased from Harlan Sprague Dawley (Indianapolis, IN). Female 5–6-week-old mice were used for all experiments. The mice were maintained in a barrier-type facility approved by the American Association for Accreditation of Laboratory Animal Care and in accordance with current regulations and standards of the United States Department of Agriculture, Department of Health and Human Services, and NIH. STn-positive tumor cell lines T47D (human ductal breast carcinoma) and SW620 (human colon carcinoma) were obtained from ATCC (Manassas, VA), and the Met129 cell line (C3H murine methylcholanthrene-induced mammary carcinoma) was kindly provided by Dr. J. Vaage (Roswell Park Memorial Institute, Buffalo, NY). The hybridoma cell line B72.3 (derived from P3X63Ag8 plasmocytoma cells producing anti-sTn IgG1) was used as a source of anti-sTn IgG1. All cell lines were maintained in medium supplemented with 10% fetal bovine serum. MH-S mouse alveolar MOs were obtained from ATCC. PMN cells were obtained from peripheral blood of SCID beige mice at a final concentration of 1.5×10^6 cells/ml.

ELISA Tests. The ELISA tests for sTn and anti-sTn IgG were made in the laboratory by combining mouse irrelevant IgG1 (Pierce, Rockford, IL), peroxidase-conjugated antimouse IgM and IgG (Sigma, St. Louis, MO), anti-sTn MAbs HB-sTn (DAKO, Carpinteria, CA), and peroxidase-conjugated B72.3. Purified B72.3 anti-sTn Ab was produced from the hybridoma cell line (ATCC). Peroxidase-conjugated B72.3 was synthesized with a Pierce kit,

Received 11/2/01; accepted 10/4/02.

The costs of publication of this article were defrayed in part by the payment of page charges. This article must therefore be hereby marked *advertisement* in accordance with 18 U.S.C. Section 1734 solely to indicate this fact.

[1] To whom requests for reprints should be addressed. Present address: 1555 Picardae Court, Powell, OH 43065. Fax: (614) 888-6946; E-mail: ebarbera@columbus.rr.com.

[2] The abbreviations used are: VEGF, vascular endothelial growth factor; MO, macrophage; PMN, polymorphonuclear; TIM, tumor-infiltrating macrophage; sTn, sialyl-Tn; Ag, antigen; SCID, severe combined immunodeficient; RT-PCR, reverse transcription-PCR; ATCC, American Type Culture Collection; m-VEGF, murine VEGF; h-VEGF, human VEGF; BSM, bovine submaxillary mucin; PE, phycoerythrin; G3PDH, glyceraldehyde-3-phosphate dehydrogenase; Ab, antibody; DAPI, 4′,6-diamidino-2-phenylindole; MAb, monoclonal Ab; TAA, tumor-associated Ag; m-MO, mouse MO; m-PMN, mouse PMN.

according to the manufacturer's instructions. The ELISA kits for m-VEGF and h-VEGF were purchased from R&D Systems (Minneapolis, MN).

Cellular Interactions for *in Vitro* VEGF Release Tests. Intercellular interaction studies were performed in 24-well plates (Becton Dickinson, San Jose, CA). For coculture experiments, the concentrations of cells and test products were adjusted as follows: MH-S MO was diluted to a final concentration of 1.5×10^6 cells/ml, equal amounts of PMN cells were adjusted (tested by Giemsa staining) and resuspended in RPMI 1640 to a final concentration of 10^6 cells/ml, and tumor cells (T47D or SW620) were diluted to a final concentration of 1.5×10^5 cells/ml. The quantity of the different additives used in the tests was as follows: (*a*) B72.3 anti-sTn Ab (purified from B72.3 hybridoma cell culture media) at 0.06 μg/well; (*b*) BSM (Sigma), a polyvalent sTn Ag, at 0.75 ng/well; (*c*) monovalent sTn Ag (sTn epitope; Calbiochem, San Diego, CA) at 30 ng/well; and (*d*) latex beads (Sigma) at 3×10^6/well.

Serum Tests. Blood samples were obtained from the tail vein (20 μl/sample). The cells were sedimented by centrifugation, and the serum was separated. The serum was diluted 1:50 in PBS containing 0.05% Tween. ELISA tests, using plates coated with sTn Ag (BSM) or anti-sTn Ab, were used to measure the serum content of specific anti-sTn IgG, anti-sTn IgM, and sTn Ag.

m-VEGF RT-PCR. VEGF transcription modification by cellular interactions (direct contact or through soluble factors) was studied in cell cultures performed on polystyrene films using OptiCell (BioCrystal, Westerville, OH). To test the VEGF production of cocultured cells, tumor cells and MOs were seeded as follows: (*a*) 5×10^5 T47D and 5×10^5 MH-S cells on the same film; and (*b*) 5×10^5 Met129 cells on one film and 5×10^5 MH-S cells on the opposite film. The cells were cultured for 72 h in RPMI 1640 supplemented with 10% fetal bovine serum. After culture, the films were separated, and 1-cm^2 fragments were cut from each film and immunostained. The cell composition on each film was tested by fluorescence microscopy staining with PE-conjugated antimouse CD11b Ab (PharMingen, San Diego, CA) as a marker for MS-H cells. Total RNA from each individual film was extracted using 1 ml of Trizol reagent (Life Technologies, Inc., Carlsbad, CA). Each total RNA (800 ng) was reverse transcribed using the SuperScript II Pre-Amplification System (Life Technologies, Inc.). PCR primers for m-VEGF were constructed by Sigma Genosys (The Woodlands, TX). Primer sequences are as follows: (*a*) VEGF-A, 5′-TCT-CTT-GGG-TGC-ACT-GGA-C and 3′-TTT-AAC-TCA-AGC-TGC-CTC-GC; (*b*) VEGF-B, 5′-CCA-GCC-ACC-AGA-AGA-AAG and 3′-GAG-TGG-GAT-GGA-TGA-TGT-C; (*c*) VEGF-C, 5′-CTG-TGC-TTC-TTG-TCT-CTG-G and 3′-CAC-ATC-TAT-ACA-CAC-CTC-ACG; and (*d*) VEGF-D, GAA-GAA-TGG-CAG-AGG-ACC and 3′-CAT-GGT-GCT-TTA-CAG-ACG. G3PDH was used as an internal control. G3PDH primers were purchased from Clontech (Palo Alto, CA). The PCR cycling protocols for VEGF and G3PDH control were as follows: 35 cycles of 7 min at 95°C, 45 s at 94°C, 45 s at 55°C, 2 min at 72°C, 10 min at 72°C, and hold at 4°C.

Tumor Production and Evaluation. Tumors were produced by s.c. injection of 10^6 tumor cells, suspended in 100 μl of PBS. Tumor growth was monitored by daily external measurement of two crossed diameters with a caliper. Samples of blood were obtained 7 days after tumor implant and after sacrifice. The serum contents of anti-sTn IgG1, anti-sTn IgM, and free sTn Ag were measured by the use of ELISA. When one diameter of the tumor reached 25 mm, the mice were sacrificed by CO_2 asphyxiation. Liver, spleen, and lungs were then removed for study. Tumors were harvested and divided into halves: one half was snap-frozen in liquid nitrogen; and the other half was fixed in formalin and embedded in paraffin. The tissue content of anti-sTn IgG1 and the free sTn Ag was analyzed in extracts of homogenized tissue by ELISA. The tissue distributions of IgG1, IgM, and sTn Ag were assessed by immunohistochemistry (immunoperoxidase). The number of metastases was counted using microscopy. Histology was assessed using standard H&E staining. In all animal experiments, the NIH principles of laboratory animal care (Principles of Laboratory Animal Care, NIH Publication No. 85-23, revised 1985) were followed, as well as specific national laws (*e.g.,* the current version of the German Law on the Protection of Animals), where applicable.

Histology and Immunohistochemistry of Human Tumors. Blocks of paraffin-embedded human colonic carcinoma tissue were kindly provided by the Department of Pathology of Memorial Hospital of Union County (Marysville, OH). Serial 3-μm-thick sections of each tumor were immunostained with peroxidase-conjugated mouse antihuman CD11b (Chemicon International, Temecula, CA), peroxidase-conjugated B72.3 mouse anti-sTn MAb, or peroxidase-conjugated mouse antihuman IgG MAb (DAKO). All sections were counterstained with hematoxylin. Digital photographs of adjacent fields were obtained, and coincidence of different stains in specific cell clusters was assessed.

Flow Cytometry. Tumors were disrupted using a combination of gentle mechanical dissociation followed by digestion with collagenase type IV (Sigma) and DNase I (Sigma) mixture. Spleens were mechanically dissociated. Spleen cells and tumor cells were isolated and immunostained with PE-conjugated anti-CD11b MAb (PharMingen). The relative amount of CD11b$^+$ cells was assessed by flow cytometry using an EPICS system (Beckman Coulter, Inc., Miami, FL).

Morphometric Analysis of Intratumor Vasculature and Cellular Infiltration. For each tumor, 10 cryostat sections (5-μm thick) were serially cut, 300 μm apart. Tumor sections were stained with both FITC-conjugated Abs to mouse CD31 (PharMingen) to visualize the vessels and PE-conjugated Abs to mouse CD11b (PharMingen) to identify MOs, and nuclei were counterstained with DAPI fluorochrome. The fluorescent and bright-field digital images of adjacent fields were recorded using a Zeiss photomicroscope (Carl Zeiss, Thornwood, NY) equipped with a TEC-470 video camera (Optronix, Goleta, CA). The digital images were analyzed with PhotoQuant image analysis software (NBG, Bilbao, Spain). Serial sections were used to determine associations between cell clusters and structures (MO clusters, tumor cell clusters, and vessels). The number of fluorescent MOs, total cells, and vessels was counted and expressed as the number of events/mm^2 tumor tissue surface area. Granulocytes were counted by nuclear morphology recognition (DAPI staining). The infiltration was expressed in cells/mm^2 tumor tissue surface area or by ratios (number of CD11b$^+$:total DAPI-stained cell number, number of CD31$^+$ events:total DAPI-stained cell number, and number of CD11b$^+$ cells: number of CD31$^+$ events).

Statistical Analysis. All statistical analyses were performed using GraphPad Prism V.2.1 (GraphPad Software Inc., San Diego, CA). The statistical significance of the results was tested by Student's *t* test (two-tailed *P*) or ANOVA, depending on the hypothesis to test. For subgroup analyses and to investigate the relationships between variables, Spearman's correlation, χ^2, Kruskal-Wallis, ANOVA, Mann-Whitney, and Student's *t* tests were used as appropriate. $P < 0.05$ was considered statistically significant.

RESULTS

Tumor-infiltrating Phagocytes Contain Phagosomes with Both TAAs and Host IgG Molecules. In an initial study, a limited number of archival human paraffin-embedded adenocarcinomas (five breast and five colon adenocarcinomas) were randomly selected. Serial sections of samples of each tumor were stained for CD11b, sTn Ag, or human IgG. In all tumors studied, abundant CD11b$^+$ MOs, plasma cells and PMN cells were observed between the tumor cells and in the reactive stroma (Fig. 1*A*). The higher concentration of these infiltrating cells was always in the interstitial stroma and in the interface tumor/normal connective tissue. A second staining using B72.3 MAb, which reacts exclusively with clustered sTn (27, 28), permitted the detection of cells containing the TAA TAG-72 (29, 30). This immunostaining (Fig. 1*B*) showed that many MOs and PMN cells surrounding tumor cell clusters harbored tumor-derived TAG-72 molecules. Serial sections stained with antihuman IgG showed that most of the phagocytes infiltrating the tumor also contained IgG in the phagosomes (Fig. 1*C*).

The Number of MOs Infiltrating the Adenocarcinoma Tissue Is Proportional to the Number of Tumor Cells. Eighteen C3H mice received a s.c. injection of 10^6 Met129 isogeneic adenocarcinoma cells. Groups of six mice were sacrificed 1, 2, and 3 weeks after the tumor challenge, and the tumors were studied. The tumor sections were immunostained with PE-conjugated anti-CD11b MAb and counterstained with DAPI. Automatic cell counts of the different tumor sections, performed with the specific computer program, showed that CD11b$^+$ cells were present throughout the entire tumor tissue and

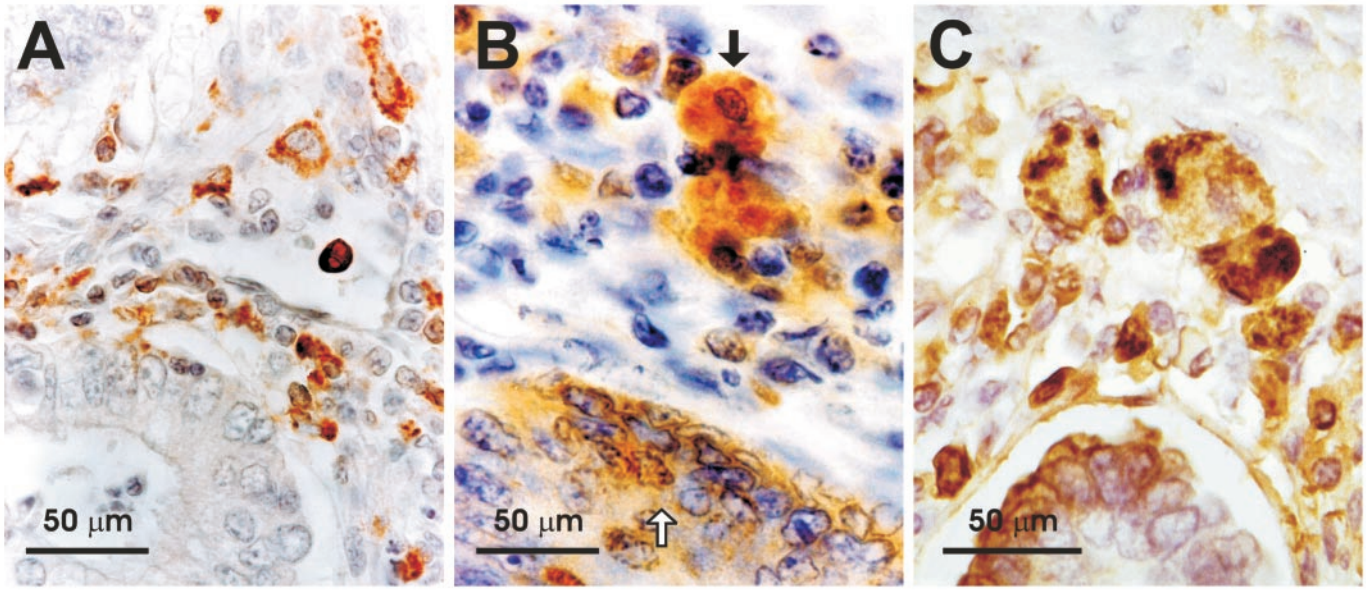

Fig. 1. Human TIMs contain TAAs and human IgG in the phagosomes. *A*, section of a TAG-72+ human colon adenocarcinoma showing heavy infiltration of $CD11b^+$ cells, including monocytes/MOs. Sections of tumor were immunostained with peroxidase-conjugated mouse antihuman CD11b. This is an average field of tumors from different patients. *B*, section of the same tumor immunostained with peroxidase-conjugated anti-sTn B72.3 MAb. Epithelial cells (*open arrows*) and infiltrating MOs (*filled arrows*) show cytoplasmic sTn Ag^+ content. *C*, parallel tumor section stained with peroxidase-conjugated mouse antihuman IgG MAb. Most sTn^+ MOs and PMN cells also contained IgG molecules. Some lymphocytes and plasma cells also show IgG^+ staining. *Bars* (50 μm) refer to the magnification of the pictures.

were mixed with tumor cells (Fig. 2*A*). Moreover, the number of total cells integrating tumor tissue was proportional to the number of $CD11b^+$ cells (Fig. 2*B*). Considering a total of 300 frames analyzed, variations of the total cells:$CD11b^+$ cells ratio were approximately 5:1 (Fig. 2*B*). It was evident that this proportion was independent of tumor size or age. The flow cytometry analyses confirmed these data. The proportion of $CD11b^+$ cells was 22–28% in all samples analyzed (30 total), independent of the size or age of tumors (Fig. 2*C*).

***In Vitro* Interaction of Tumor Cells and MOs Enhances the MO Release of VEGF.** Tumor cell-MO interactions in the tumor microenvironment may result in different consequences such as tumor cell death and/or the release of inflammatory cytokines and VEGF (31, 32). To test whether interactions of tumor cells and MOs changed the pattern of VEGF production, an *in vitro* assay was developed in which tumor cells and MOs were cocultured, and the VEGF release into the media was monitored within a 48-h period. In that model, the tumor cells were human (T47D breast adenocarcinoma and SW620 colon carcinoma), and the MOs were murine. h-VEGF and m-VEGF were differentiated using specific MAb with no cross-reactivity. That strategy allowed the discrimination of tumor cell or MO origin of the VEGF released into the media. Two types of cocultures were tested: (*a*) tumor cells and MOs (or others) in contact; and (*b*) tumor cells and MOs (or others) not in contact but sharing the media. These experiments demonstrated that the tumor cells secrete VEGF in detectable amounts (Fig. 3*A*). We tested several murine cell types including MOs, latex-activated MOs, PMN cells, and the plasmocytoma cell line P3X63Ag8. Only the MOs secreted considerable amounts of VEGF even when cultured alone. In this experiment, the amount of VEGF secreted by the MOs was always 2–3 times higher than the amount of VEGF secreted by those specific tumor cells (Fig. 3, *A* and *B*). When MOs and tumor cells were cocultured in contact or sharing soluble factors, the tumor cells never altered their pattern of VEGF secretion (Fig. 3*C*). However, the MOs in the presence of tumor cells always increased secretion of VEGF by a factor of 2 or 3 over the MO baseline (Fig. 3*D*). The consequence of that increase was that the final VEGF produced by the MOs was 5–6 times the VEGF produced by tumor cells (Fig. 3, *C* and *D*). To test whether the PMN cells in the inflammatory infiltrate could affect the amount of VEGF release into the tumor microenvironment, proportional numbers of murine PMN cells were added to MO cultures and to MO/tumor cell cocultures. PMN cells alone did not secrete significant amounts of VEGF (Fig. 3, *B* and *D*). MOs augmented by a statistically significant 20–35% the amount of m-VEGF released into the media in the presence of PMN cells. Addition of tumor cells into cultures containing MOs and PMN

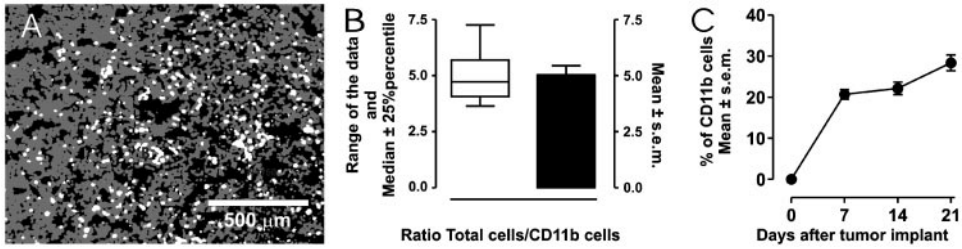

Fig. 2. Magnitude of MO infiltration of tumor tissue. *A*, digital image of the center of a 21-day-old tumor. $CD11b^+$ cells (*white spots*) were dispersed among growing tumor cells (*gray spots*). *B*, accumulated cell counts of 300 digital fluorescence microscopy fields from sections of 7-, 14-, and 21-day-old tumors (6 tumors of each age). Sections were double-stained with PE-conjugated anti-CD11b Ab and DAPI. The total cells:$CD11b^+$ cells ratio shows narrow SD. *C*, cells isolated from samples of 7-, 14-, and 21-day-old tumors. Flow cytometry analysis of cells isolated from samples of the same tumors showing a constant proportion $CD11b^+$ cells:total cells from day 7 until day 21, despite the progressive growth of the tumor mass (average of tumor tissue: day 7 = 5 mg; day 21 = 500 mg). Results are the average of 10 organs and 3 repeated flow cytometry analyses/organ (n = 30). *Bars*, SE.

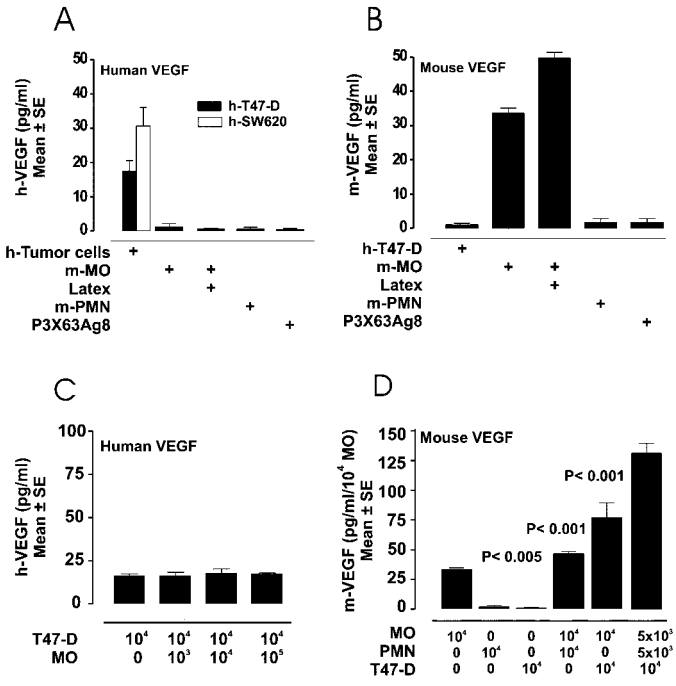

Fig. 3. Production of VEGF by cultured carcinoma, plasmocytoma, PMN, and MO cell lines. *A*, m-MO, mouse phagocytosis-activated MOs (*Latex*), m-PMN cells, mouse plasmocytoma cells (*P3X63Ag8*), and human tumor cells (*h-Tumor cells* and *h-T47-D*) were cultured separately. Only human tumor cell lines were positive for h-VEGF ELISA test. *B*, ELISA test for m-VEGF. Human tumor cell cultures were negative. All m-MO cultures showed the presence of VEGF. The addition of latex beads enhanced the m-MO release of VEGF. *C*, T47D human tumor cells cocultured with different concentrations of m-MO. The supernatants were tested by ELISA for h-VEGF and showed that the presence of MO does not change tumor cell VEGF production. *D*, m-VEGF ELISA results of T47D cells, m-MO, or m-PMN cultured alone and cocultures of m-MO + m-PMN and m-MO + m-PMN + T47D tumor cells. The cocultures m-MO + m-PMN and m-MO + T47D showed a statistically significant increase in VEGF release. The presence of tumor cells in the mixture m-MO + m-PMN introduced an additional increment of m-VEGF. All *bars* represent the average of three separate experiments and 3 ELISA evaluations/experiment ($n = 9$). Significance between averages is shown as *P*.

cells increased the amount of m-VEGF released into the media by 400–500% over the MO baseline (Fig. 3*D*).

The Pattern of VEGF Transcription Was Altered in Tumor Cells but not in MOs When Both Interacted in the Same Environment. To test whether tumor cell-MO interaction could alter patterns of VEGF mRNA expression of either cell type, several models of cocultures were tested. MOs cultured alone showed a repetitive pattern: VEGF-A and VEGF-B mRNA were present, but VEGF-C or VEGF-D were not (Fig. 4*A*). MOs cocultured with tumor cells, in contact or separated, showed the consistent presence of VEGF-A and VEGF-B mRNA, but not VEGF-C or VEGF-D (Fig. 4, *B*−*D*). When cultured alone or in the presence of MOs, tumor cells showed all four types of VEGF mRNA (Fig. 4*E*). However, in growing Met129 tumors, VEGF-C mRNA was not detectable (Fig. 4*F*).

In Growing Tumors, Neoangiogenesis Was Predominant in Areas of MO Concentration. To test the possible association between MO infiltration and tumor neoangiogenesis, Met129 tumor cells were injected s.c. in groups of mice. These mice were sacrificed when the tumors were 5 and 10 mm in diameter. Tumors were excised together with surrounding tissues to maintain intact histology of tumor borders. Serial sections were triple-stained with DAPI (to use as a nuclear reference), PE-conjugated anti-CD11b MAb (to detect MOs), and FITC-conjugated anti-CD31 MAb (to detect endothelial cells). A computerized analysis was done on 300 color video images of 30 tumor sections. The red:blue fluorescence ratio was determined as an expression of the ratio of MOs to total cells. In early tumors (5 mm in diameter), the MOs were predominantly concentrated on tumor borders, especially at the interface between the growing mass of tumor cells and s.c. connective tissue (Fig. 5*A*). $CD31^+$ cell concentration was parallel to the MO concentration, forming capillaries with a predominant orientation toward the center of the tumor mass, in the same direction as the MO gradient (Fig. 5*B*). In advanced tumors (10 mm in diameter), MOs were highly concentrated in the periphery of large vessels in perivascular connective tissue (Fig. 5*C*), suggesting that this area assumed the role of the interface observed in early tumors. The $CD31^+$ cells followed parallel distribution to MO clusters and were more concentrated in the periphery of large vessels, projecting capillaries toward the tumor center (Fig. 5*D*).

The sTn Ag and IgG against It Can Stimulate an Increase of MO VEGF Release. Previously, we observed that IgG against TAAs could stimulate tumor invasion and metastasis (31), mediated by a cooperation of PMN cells and MOs activated by IgG^+ Ag complexes (32). Based on these published data and the association of TIMs with TAAs and host IgG observed in human tumors, we studied whether both TAAs and Abs raised against these Ags could modulate the MO-derived VEGF release. Using an *in vitro* model, two human tumor cell lines (breast T47D and colon SW620 cells) that secrete sTn TAA were selected (Fig. 6*A*). The secreted Ag was captured from the cell culture supernatant in a column or by immunoprecipitation using B72.3 MAb. Immobilized Ag was further detected by peroxidase-conjugated B72.3 Mab, showing, as known, the existence of multiple repeated epitopes on the same molecule/conglomerate of Ag released by the tumor cells (repeated epitope Ag). Additionally, it was confirmed that neither murine MOs nor murine PMN cells released such Ag (Fig. 6*A*). Bovine salivary mucin, a repeated epitope sTn Ag, and

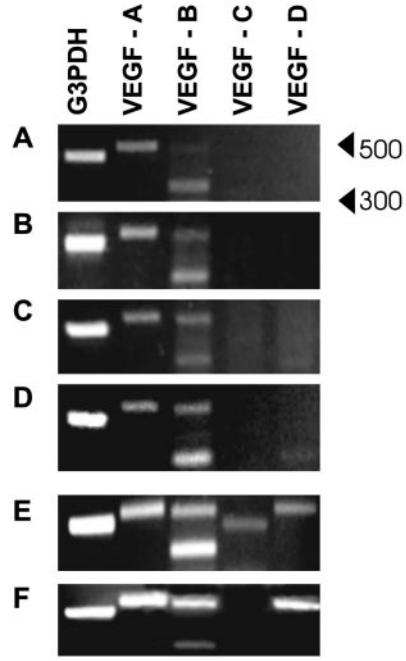

Fig. 4. Pattern of VEGF transcription of m-MO interacting in the same environment with tumor cells. *A*, MS-H cells (m-MO) cultured alone showed a repetitive pattern of VEGF transcription: VEGF-A and VEGF-B mRNA were present, but VEGF-C and VEGF-D mRNA were not. *B*, MH-S cells cultured in contact with human tumor cells (T47D cells) showed the same pattern of VEGF transcription. *C*, MH-S cells cocultured in the same media environment but not in contact with T47D cells showed the same repetitive pattern of VEGF transcription. *D*, MH-S cells cocultured in the same environment but not in contact with mouse tumor cells (Met129 cells) showed the same repetitive pattern of VEGF transcription. *E*, Met129 cells cultured alone showed expression of VEGF-A, -B, -C, and -D mRNA. *F*, VEGF mRNA extracted from s.c., growing Met129 tumors (six tumors). VEGF-C disappeared. All RT-PCR tests were repeated 6 times/experiment.

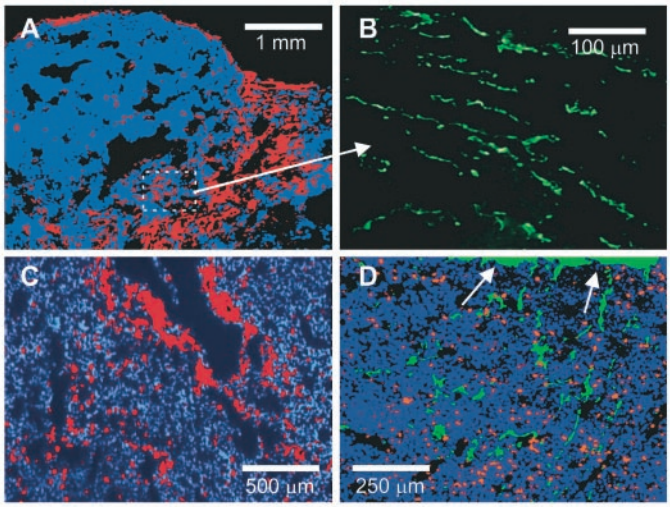

Fig. 5. Association between TIMs and tumor angiogenesis. *A*, fluorescence image of early tumor (7 days after implant, 5 mm in diameter), sectioned vertically to show the base of implantation, invasion, and growth in the s.c. tissues. MOs (*red*) were stained with PE-conjugated anti-CD11b MAb, and all cell nuclei were stained with DAPI (*blue*). The highest concentrations of MOs (*red areas*) were always in the tumor tissue-normal tissue interface, in the front of invasion of the tumor, and together with growing mature vessels. *B*, higher magnification of the area *boxed* in *A*. Endothelial cells are shown (*green*). This is an example of neoangiogenesis penetrating tumor tissue from mature vessels of the interface tumor tissue-normal tissue. *C*, immunofluorescent image of a tumor section stained with PE-conjugated anti-CD11b MAb and counterstained with DAPI. More concentrated $CD11b^+$ infiltration (*red*) was observed surrounding the tumor vascular structures. *D*, image of the section of *C* showing detail of $CD11b^+$ (*red*) and endothelial cell distribution (*green*, stained with fluorescein-conjugated anti-CD31 MAb). Close to the periphery of the endothelial cells of the vascular structure (*top green area with arrows*), new capillaries (*green*) were among $CD11b^+$ cells (*red*).

a synthetic single epitope sTn Ag were used as controls for *in vitro* experiments. When tumor cells (secreting sTn) were cultured alone in the presence of B72.3 Mab, with the single epitope sTn Ag, or with both together, the amount of VEGF released into the media in 48 h was not changed. Therefore, the presence of anti-tumor-associated Ab did not modulate the tumor cell VEGF release (Fig. 6*B*). The presence of single epitope sTn Ag or anti-sTn IgG did not change the release of MO-derived VEGF in 48 h compared with the controls. However, it was noted that MOs cultured in the presence of repeated epitope sTn Ag increased VEGF release in 48 h (Fig. 6*C*). Addition of both repeated epitope sTn Ag and anti-sTn IgG produced the same effect as repeated epitope sTn Ag alone (Fig. 6*C*). Cocultures containing MOs, PMN cells, and T47 D tumor cells showed that in the presence of tumor cells (tumor cells and sTn Ag secreted by the tumor cells), MOs increased the release of VEGF in 48 h (Fig. 6*D*). Also consistent with previous experiments, the addition of anti-sTn IgG did not change the amount of MO VEGF released in the presence of tumor cells and sTn Ag (Fig. 6*D*). Notably, the presence of tumor cells in cocultures of MOs and PMN cells dramatically increased the MO release of VEGF (Fig. 6*D*). Significantly, when anti-sTn IgG was added to cultures of MOs in the presence of tumor cells with their own shed sTn Ag and PMN cells, in 48 h the amount of MO-secreted VEGF increased 500% over the normal production (Fig. 6*D*).

MO Infiltration and Tumor Angiogenesis Are Correlated with the Amount of Anti-TAA IgG Present in the Host. To analyze the *in vivo* consequences of the data shown above, the density of $CD11b^+$ cells and capillaries generated (using immunofluorescence staining with fluorescein-conjugated antimouse CD31) were measured in T47D tumors growing in SCID mice and *nu/nu* mice. In an experimental model of SCID mice growing T47-D sTn^+ tumors, no anti-sTn IgG was present in serum. In this model, tumors grew slowly and showed very few new vessels (Fig. 7, *A* and *B*), and the number of MO clusters was parallel to the number of vessels and the number of tumor cells. In a group of six SCID mice of this model, s.c. injection of 150 μg of irrelevant IgG did not introduce differences in tumor angiogenesis or tumor growth. However, a group of these mice, which received a s.c. injection of 150 μg of B72.3 Mab, showed a very significant increase of serum anti-sTn IgG (exogenous), new tumor vessels (Fig. 7*A*), and a proportional number of MOs. Those tumors showed a significantly faster tumor growth (Fig. 7*B*). A second model of *nu/nu* mice growing T47D sTn^+ tumors showed results consistent with the above data. In the serum of the *nu/nu* mice, there were significant

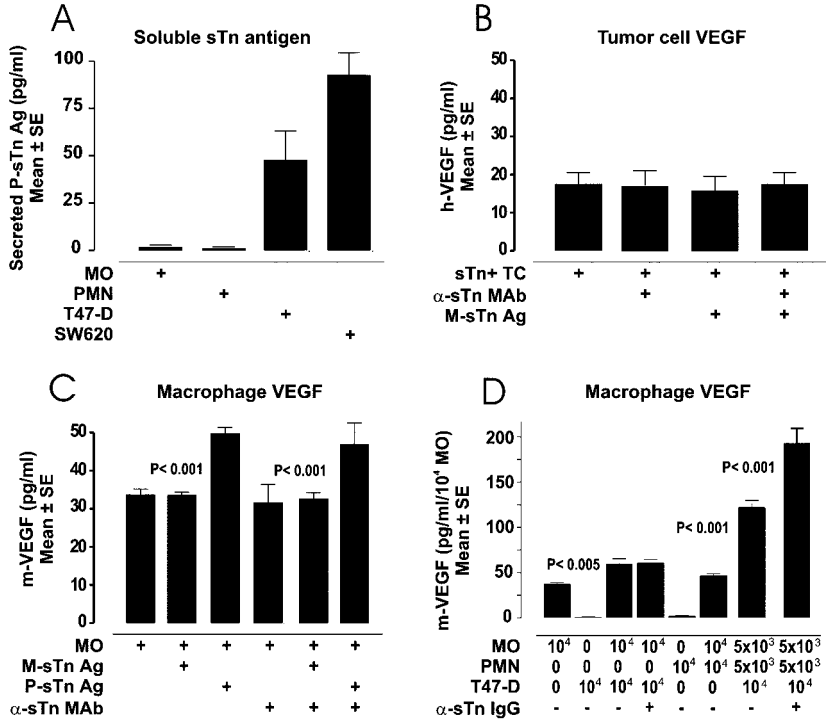

Fig. 6. VEGF production of cultured tumor cells or MOs in the presence of shed/secreted TAA sTn and/or anti-sTn IgG. *A*, sTn TAA released by T47D or SW620 human tumor cells, m-MOs, or m-PMN cells cultured for 48 h. The sTn Ag content in the supernatant assessed by ELISA test showed that only tumor cells secreted the sTn Ag. *B*, h-VEGF ELISA results from the supernatant of T47D cells secreting sTn Ag (*sTn + TC*) cultured in media with B72.3 MAb (*α-sTn MAb*), single epitope sTn Ag (*M-sTn Ag*), or both. The tests showed that the presence of these molecules does not modify the tumor cell VEGF secretion. *C*, m-VEGF ELISA from supernatant of MOs cultured in media supplemented with single epitope sTn Ag (*M-sTn Ag*), polyvalent sTn Ag BSM (*P-sTn Ag*), B72.3 MAb (*α-sTn MAb*), or combinations. A statistically significant increase in VEGF release was shown when tumor cells were cultured in the presence of polyvalent sTn Ag. In these conditions the addition of anti-sTn IgG does not modify MO VEGF production. *D*, m-VEGF ELISA results of T47D cells, m-MOs, or m-PMN cells cultured alone and cocultures of PMN and MO + PMN + T47D tumor cells in media with and without anti-sTn IgG. A statistically significant increase in VEGF release was shown when MOs were cultured in the presence of tumor cells. The presence of tumor cells in the MO + PMN mixture induces higher production of MO-derived VEGF, and the addition of B72.3 MAb (*α-sTn IgG*) induces the highest release of MO-derived VEGF. All *bars* represent the average results of three separate experiments and 3 ELISA evaluations (wells)/experiment ($n = 9$). Significance between averages is shown as *P*.

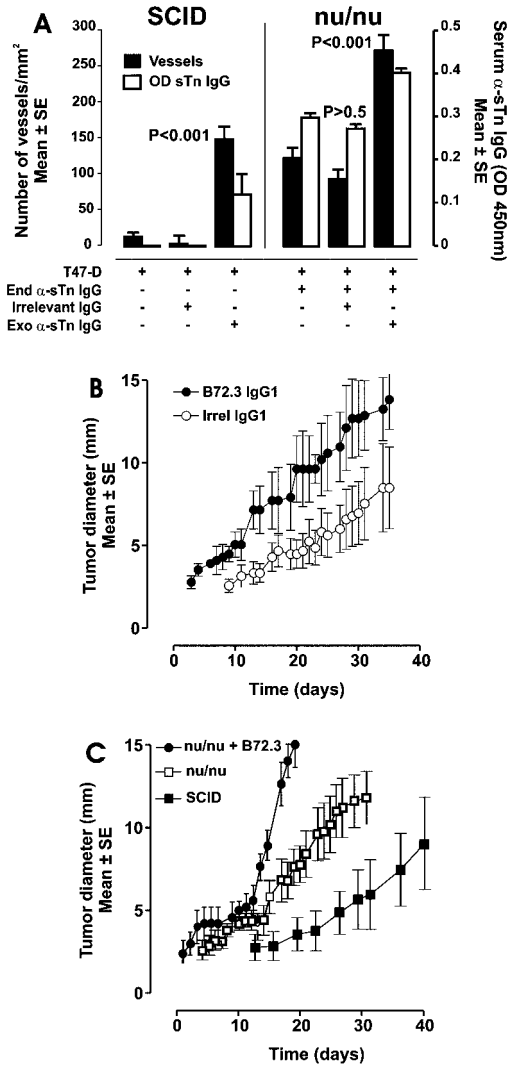

Fig. 7. Comparative tumor angiogenesis and tumor growth in the presence or absence of anti-sTn IgG in the host. *A*, in SCID mice, tumor cells grew without host endogenous IgG response (*End α-sTn IgG). Tumors grew with insignificant angiogenesis (number of vessels/mm*^{2}, ■*). Injection of exogenous irrelevant IgG (*Irrelevant IgG*) did not change the pattern of tumor angiogenesis. The injection of B72.3 MAb (*Exo α-sTn IgG) resulted in a significant increase of serum α-sTn IgG (serum α-sTn IgG, □) and a very significant increase of tumor angiogenesis. In *nu/nu* mice, a low level of endogenous serum α-sTn IgG existed, and tumor angiogenesis was important. The injection of exogenous irrelevant IgG did not change the pattern of tumor angiogenesis. The injection of B72.3 MAb resulted in a significant increase of both serum α-sTn IgG and tumor angiogenesis. All *bars* represent the average result of six mice ($n = 6$) and 3 ELISA evaluations/mouse ($n = 18$). Significance between averages is shown as *P*. *B*, pattern of tumor growth in SCID mice. In mice with exogenous irrelevant IgG but not α-sTn MAb (○), the tumors grew more slowly than those in mice receiving exogenous α-sTn MAb (B72.3 IgG, ●). *C*, pattern of tumor growth in SCID *versus nu/nu* mice. In SCID mice with exogenous irrelevant IgG but not α-sTn MAb (■), the tumors grew more slowly than those in *nu/nu* mice with exogenous irrelevant IgG and endogenous α-sTn MAb (□). *nu/nu* mice receiving supplementary exogenous α-sTn MAb (B72.3 IgG, ●) showed a significant increase of tumor growth. All *dots* represent the average results from six mice ($n = 6$). *Bars*, SE.

titers of endogenously generated anti-sTn IgG (Fig. 7*A*). Tumors of this model showed higher concentrations of new vessels and faster growth (Fig. 7, *A* and *C*). The s.c. injection of 150 μg of irrelevant IgG in these mice did not introduce significant changes in MO infiltration, vessel density, or tumor growth (Fig. 7*A*). However, the group of mice that received s.c. injection of 150 μg of B72.3 MAb (exogenous anti-sTn IgG) showed a very significant increase of serum anti-sTn IgG, new tumor vessels (Fig. 7*A*), and a proportional number of MOs (data not shown). The tumor growth was significantly faster during the last 7 days of the experiment (Fig. 7*C*).

DISCUSSION

The results presented here suggest that the TIMs have an important role in promoting tumor angiogenesis, maintaining tumor growth, the invasive course of malignant tumors, and facilitating the metastasis cascade. In addition, formation of immune complexes in tumor connective matrix appears to be a complementary mechanism of MO and PMN cell attraction into the tumor tissue. Since the discovery of the capacity of tumor cells to produce VEGF, it has been broadly assumed that the tumor cell drives vessel formation in growing neoplastic tissue (33, 34).

Independently of this assumption, experiments inhibiting critical angiogenic factors such as VEGF demonstrate that neoangiogenesis is a bottleneck in the malignant process; by impairing angiogenesis, tumor growth could be totally suppressed (35–37). Because the majority of tumor cells express angiogenic factors, it can be assumed that the tumor cell is necessary and sufficient to sustain the neoangiogenesis that autoensures tumor growth. However, there is a certain discrepancy in accepting the predominant role of the tumor cell supplying sufficient vascular stimulating factors for effective tumor neoangiogenesis. Other normal cells involved in the tumor biology such as monocytes and platelets may import considerable amounts of VEGF into critical points of the tumor (38–40). MOs are capable of producing and releasing VEGF under the influence of certain factors such as hypoxia and nitric oxide, both common factors of the tumor environment (41). Actually, high VEGF expression has been frequently observed in TIMs (42), and increased tumor angiogenesis has been reported after MO recruitment into the tumor (23).

TIMs are common and abundant (43) and are frequently interpreted as representative of antitumor activity (44). However, here and in other published studies (45), our histology results cannot sustain an important tumor cytolysis due to the infiltrating MOs. Actually, our results show that the TIMs are mainly concentrated in the interphase between the tumor and normal tissue and, in general, are associated with phagocytosis of tumor cell debris and immune complexes containing TAAs. This suggests that in the tumor environment, the MO is acting more as a scavenger cell than as a cytotoxic/cytolytic cell. Our substantial morphometric and flow cytometry analyses show that the number of MOs infiltrating the tumor mass in experimental tumors is proportional to tumor volume and that during the exponential phase of tumor growth a ratio of tumor cells:MO remains practically constant. Considering both observations together strongly reinforces the concept that the MOs may play an essential role in promoting tumor growth (23). *In vivo*, MO recruitment into the tumor could be driven by multiple factors including hypoxia, MO or tumor cell production of chemokines (46–48), and accumulation of cell debris and/or immune complexes in the tissue microenvironment (49, 50). The repetitive presence of MOs with endocytosed material containing TAA and anti-TAA IgG in human tumors, together with our *in vitro* results, supports the possibility that in the *in vivo* tumor environment, both phagocytosis of cell debris and the presence of immune complexes (formed with TAA and anti-TAA IgG) may promote the secretion of very important amounts of VEGF by infiltrating MOs. The frequent association of MOs with PMN cell and plasma cell infiltration, mainly observed at the tumor boundaries, suggests that a concomitant inflammation follows MO recruitment into the tumor cell invasive front. Immune complexes involving shed TAA and antitumor IgG may activate this inflammatory cellular infiltrate, stimulating the local secretion of proinflammatory cytokines and establishing a feedback process of infiltration-activation (31). The *in vitro* tests also showed that tumor cells could stimulate the secretion of MO VEGF and not *vice versa*. No experiments were done to uncover the molecular nature of factors involved in this stimulus, but the results showed that tumor

cell-MO contact is not needed to provoke this MO response. RT-PCR analysis of the MO mRNA before and after such stimulus showing the same pattern of VEGF gene expression (VEGF-A and -B were expressed, but not VEGF-C or -D) suggests that the VEGF MO response was quantitative but not qualitative. A tumor cell type capable of expressing VEGF-A, -B, -C, and -D *in vitro* inhibited the expression of VEGF-C, which is supposedly involved in promoting lymphatic angiogenesis, when growing *in vivo* (51, 52). This VEGF-C-specific inhibiting phenomenon could be anecdotal of this tumor cell type but essentially illustrates that tumor cells could alter their pattern of VEGF expression depending on microenvironmental factors. Importantly, the *in vitro* coculture experiments involving MO, PMN cells, and tumor cells strongly suggest that in the tumor, within the cellular inflammatory environment, each MO can secrete much more VEGF than certain tumor cells, which substantiates the importance of TIMs as a source of VEGF in the tumor tissue. In normal tissue repair, it has been demonstrated that the recruitment of MOs constitutes the main source of VEGF and the fundamental step for the establishment of effective angiogenesis (53). In experimental s.c. injected tumors, our results showed that in early stages of tumor growth, the MO concentration and capillary development were always coincidental (statistically significant, $P < 0.001$, positive correlation between number of CD11b cells/number CD31 structures/field). Actually, the images suggested that tumor cells were growing toward the MO/capillary-rich areas, in an expansive/invasive progression.

Consistent with this pattern, in advanced tumors (10 mm in diameter), large tumor vessels with well-formed walls assume the role of the s.c. connective tissue interface observed in the early tumors. The new capillary formation was always close to MO clusters, concentrated in the periphery of the large vessels and projecting radial branches toward the tumor center. Both sets of data emphasize that tumor cells grow, invading the well-vascularized reactive stroma (54) and not that the stroma infiltrates the tumor cell clusters.

If the reactive stroma can support tumor growth, the identification of mechanisms capable of triggering and sustaining a stroma reaction is very important. Cytokines and other factors released by the tumor cells could be initiators. In our experiments, molecules identified by the immune system as TAAs were one kind of these tumor-released factors. The example of the common tumor-associated sTn Ag was illustrative. Complexes of molecules with repeated sTn epitopes and B72.3 IgG activate the MO VEGF response, probably through the FcγRI receptor, as demonstrated previously (31, 32). B72.3 IgG alone did not increase the MO VEGF release, showing that the presence of monomeric IgG does not induce that MO response. However, immune complexes formed with sTn-presenting molecules and specific IgG act as moderate stimulators of the MO VEGF response and also as strong inducers of MO inflammatory response (32), which may attract PMN cell infiltration. The *in vitro* experiments suggest that the concurrence of tumor cells shedding antigenic debris, the specific antitumor Ag IgG, and infiltrating PMN cells can dramatically increase the MO release of VEGF. Therefore, the locally concentrated immune complexes composed by shed tumor Ags and the specific IgG could represent a fundamental primer and/or maintainer of stroma activation, which can support tumor growth (55). The results from the *in vivo* experiments are consistent with these interpretations. The number of capillaries/unit of tumor volume and the daily growth rate of tumors were related to the serum concentration of anti-sTn IgG. Tumors growing in SCID mice, which do not develop specific IgG response, had very low vascular network and very slow growth. However, tumors growing in SCID mice injected with exogenous B72.3 IgG, specific for the TAA sTn, showed much higher capillary density and faster tumor growth. Such a tumor-enhancing effect was not observed in SCID mice injected with the same doses of irrelevant IgG isotype, which proves that increase of angiogenesis is related to the specific recognition of TAAs by the specific IgG. Moreover, *nu/nu* mice capable of developing a B-cell response, mainly IgM based, produced a certain serum concentration of endogenous anti-sTn IgG, and these mice developed tumors with a significantly higher density of capillaries as compared with tumors developed in SCID mice. With identical numbers and classes of tumor cells implanted in *nu/nu* beige mice or in SCID beige mice, tumors grew faster in *nu/nu* mice. When *nu/nu* mice had an exogenous source of B72.3 Ab supplied by injection, the results showed a higher concentration of serum anti-sTn IgG and dramatically increased the tumor vascularization. That effect was also specific because the same carcinoma growing in *nu/nu* mice injected with irrelevant IgG had the same capillary density as the controls. Neither of these mouse types, SCID or *nu/nu* beige, have natural killer cells or effective T cells. Therefore, the difference in tumor growth cannot be attributed to a different tumor rejection capacity. The only possible effectors for tumor rejection in these mouse types are the MOs and the PMN cells. However, the microscopy examination showed no suspicion of efficient tumor rejection associated with stromal cell infiltration. On the contrary, the stromal cell infiltrate was always associated with neoangiogenesis. *In vitro* data suggest that immune complexes involving shed tumor Ags and specific IgG constitute a powerful enhancer of VEGF production by stromal cell infiltrate. Considering that those immune complexes can also induce the release of chemoattractant factors by stromal cells, it is understandable that the immune complexes could further sustain tumor infiltration by more stromal cells, establishing a feedback process of infiltration-inflammation-angiogenesis. All these data suggest that tumor growth could be maintained, at least in part, by the humoral immune response against shed TAAs that may promote recruitment of stromal cells in the tumor milieu and MO production of inflammatory and angiogenic factors including high amounts of VEGF (31, 32). To address possible therapeutic implications, it is key to know how important this tumor-promoting host response is in the biology of human tumors. Many clinical data suggest that the humoral immune response against tumor Ags does not represent an effective tumor cell rejection process, and historically, the value of such a response has been considered puzzling (56, 57).

REFERENCES

1. Yoshikawa, T., Tsuburaya, A., Kobayashi, O., Sairenji, M., Motohashi, H., Yanoma, S., and Noguchi, Y. Plasma concentrations of VEGF and bFGF in patients with gastric carcinoma. Cancer Lett., *153:* 7–12, 2000.
2. Komorowski, J., Jankewicz, J., and Stepien, H. Vascular endothelial growth factor (VEGF), basic fibroblast growth factor (bFGF) and soluble interleukin-2 receptor (sIL-2R) concentrations in peripheral blood as markers of pituitary tumours. Cytobios, *101:* 151–159, 2000.
3. Edgren, M., Lennernas, B., Larsson, A., and Nilsson, S. Serum concentrations of VEGF and b-FGF in renal cell, prostate and urinary bladder carcinomas. Anticancer Res., *19:* 869–873, 1999.
4. Fuhrmann Benzakein, E., Ma, M. N., Rubbia Brandt, L., Mentha, G., Ruefenacht, D., Sappino, A. P., and Pepper, M. S. Elevated levels of angiogenic cytokines in the plasma of cancer patients. Int. J. Cancer, *85:* 40–45, 2000.
5. Detmar, M., Velasco, P., Richard, L., Claffey, K. P., Streit, M., Riccardi, L., Skobe, M., and Brown, L. F. Expression of vascular endothelial growth factor induces an invasive phenotype in human squamous cell carcinomas. Am. J. Pathol., *156:* 159–167, 2000.
6. Kondo, Y., Arii, S., Mori, A., Furutani, M., Chiba, T., and Imamura, M. Enhancement of angiogenesis, tumor growth, and metastasis by transfection of vascular endothelial growth factor into LoVo human colon cancer cell line. Clin. Cancer Res., *6:* 622–630, 2000.
7. Lewin, M., Bredow, S., Sergeyev, N., Marecos, E., Bogdanov, A., Jr., and Weissleder, R. *In vivo* assessment of vascular endothelial growth factor-induced angiogenesis. Int. J. Cancer, *83:* 798–802, 1999.
8. Aonuma, M., Saeki, Y., Akimoto, T., Nakayama, Y., Hattori, C., Yoshitake, Y., Nishikawa, K., Shibuya, M., and Tanaka, N. G. Vascular endothelial growth factor overproduced by tumour cells acts predominantly as a potent angiogenic factor contributing to malignant progression. Int. J. Exp. Pathol., *80:* 271–281, 1999.
9. Williams, C. S., Tsujii, M., Reese, J., Dey, S. K., and DuBois, R. N. Host cyclooxygenase-2 modulates carcinoma growth. J. Clin. Investig., *105:* 1589–1594, 2000.

10. Decaussin, M., Sartelet, H., Robert, C., Moro, D., Claraz, C., Brambilla, C., and Brambilla, E. Expression of vascular endothelial growth factor (VEGF) and its two receptors (VEGF-R1-Flt1 and VEGF-R2-Flk1/KDR) in non-small cell lung carcinomas (NSCLCs): correlation with angiogenesis and survival. J. Pathol., *188:* 369–377, 1999.
11. Nagashima, G., Suzuki, R., Hokaku, H., Takahashi, M., Miyo, T., Asai, J., Nakagawa, N., and Fujimoto, T. Graphic analysis of microscopic tumor cell infiltration, proliferative potential, and vascular endothelial growth factor expression in an autopsy brain with glioblastoma. Surg. Neurol., *51:* 292–299, 1999.
12. Rossler, J., Breit, S., Havers, W., and Schweigerer, L. Vascular endothelial growth factor expression in human neuroblastoma: up-regulation by hypoxia. Int. J. Cancer, *81:* 113–117, 1999.
13. Danielsen, T., and Rofstad, E. K. The constitutive level of vascular endothelial growth factor (VEGF) is more important than hypoxia-induced VEGF up-regulation in the angiogenesis of human melanoma xenografts. Br. J. Cancer, *82:* 1528–1534, 2000.
14. O'Reilly, M. S., Holmgren, L., Shing, Y., Chen, C., Rosenthal, R. A., Moses, M., Lane, W. S., Cao, Y., Sage, E. H., and Folkman, J. Angiostatin: a novel angiogenesis inhibitor that mediates the suppression of metastases by a Lewis lung carcinoma. Cell, *79:* 315–328, 1994.
15. Cameron, M. D., Schmidt, E. E., Kerkvliet, N., Nadkarni, K. V., Morris, V. L., Groom, A. C., Chambers, A. F., and MacDonald, I. C. Temporal progression of metastasis in lung: cell survival, dormancy, and location dependence of metastatic inefficiency. Cancer Res., *60:* 2541–2546, 2000.
16. Sawatsubashi, M., Yamada, T., Fukushima, N., Mizokami, H., Tokunaga, O., and Shin, T. Association of vascular endothelial growth factor and mast cells with angiogenesis in laryngeal squamous cell carcinoma. Virchows Arch., *436:* 243–248, 2000.
17. Dankbar, B., Padro, T., Leo, R., Feldmann, B., Kropff, M., Mesters, R. M., Serve, H., Berdel, W. E., and Kienast, J. Vascular endothelial growth factor and interleukin-6 in paracrine tumor-stromal cell interactions in multiple myeloma. Blood, *95:* 2630–2636, 2000.
18. Torisu, H., Ono, M., Kiryu, H., Furue, M., Ohmoto, Y., Nakayama, J., Nishioka, Y., Sone, S., and Kuwano, M. Macrophage infiltration correlates with tumor stage and angiogenesis in human malignant melanoma: possible involvement of TNF-α and IL-1α. Int. J. Cancer, *85:* 182–188, 2000.
19. Gavin, T. P., Spector, D. A., Wagner, H., Breen, E. C., and Wagner, P. D. Nitric oxide synthase inhibition attenuates the skeletal muscle VEGF mRNA response to exercise. J. Appl. Physiol., *88:* 1192–1198, 2000.
20. Richardson, R. S., Wagner, H., Mudaliar, S. R., Henry, R., Noyszewski, E. A., and Wagner, P. D. Human VEGF gene expression in skeletal muscle: effect of acute normoxic and hypoxic exercise. Am. J. Physiol., *277:* H2247–H2252, 1999.
21. Steinbrech, D. S., Mehrara, B. J., Chau, D., Rowe, N. M., Chin, G., Lee, T., Saadeh, P. B., Gittes, G. K., and Longaker, M. T. Hypoxia upregulates VEGF production in keloid fibroblasts. Ann. Plast. Surg., *42:* 514–519, discussion, 519–520, 1999.
22. Edelman, J. L., Castro, M. R., and Wen, Y. Correlation of VEGF expression by leukocytes with the growth and regression of blood vessels in the rat cornea. Investig. Ophthalmol. Vis. Sci., *40:* 1112–1123, 1999.
23. Goede, V., Brogelli, L., Ziche, M., and Augustin, H. G. Induction of inflammatory angiogenesis by monocyte chemoattractant protein-1. Int. J. Cancer, *82:* 765–770, 1999.
24. Frank, S., Stallmeyer, B., Kampfer, H., Kolb, N., and Pfeilschifter, J. Nitric oxide triggers enhanced induction of vascular endothelial growth factor expression in cultured keratinocytes (HaCaT) and during cutaneous wound repair. FASEB J., *13:* 2002–2014, 1999.
25. Levitas, E., Chamoun, D., Udoff, L. C., Ando, M., Resnick, C. E., and Adashi, E. Y. Periovulatory and interleukin-1β-dependent up-regulation of intraovarian vascular endothelial growth factor (VEGF) in the rat: potential role for VEGF in the promotion of periovulatory angiogenesis and vascular permeability. J. Soc. Gynecol. Investig., *7:* 51–60, 2000.
26. El Awad, B., Kreft, B., Wolber, E. M., Hellwig Burgel, T., Metzen, E., Fandrey, J., and Jelkmann, W. Hypoxia and interleukin-1β stimulate vascular endothelial growth factor production in human proximal tubular cells. Kidney Int., *58:* 43–50, 2000.
27. Itzkowitz, S. H., Yuan, M., Montgomery, C. K., Kjeldsen, T., Takahashi, H. K., Bigbee, W. L., and Kim, Y. S. Expression of Tn, sialosyl-Tn, and T antigens in human colon cancer. Cancer Res., *49:* 197–204, 1989.
28. Zhang, S., Walberg, L. A., Ogata, S., Itzkowitz, S. H., Koganty, R. R., Reddish, M., Gandhi, S. S., Longenecker, B. M., Lloyd, K. O., and Livingston, P. O. Immune sera and monoclonal antibodies define two configurations for the sialyl Tn tumor antigen. Cancer Res., *55:* 3364–3368, 1995.
29. Thor, A., Ohuchi, N., Szpak, C. A., Johnston, W. W., and Schlom, J. Distribution of oncofetal antigen tumor-associated glycoprotein-72 defined by monoclonal antibody B72.3. Cancer Res., *46:* 3118–3124, 1986.
30. Sheer, D. G., Schlom, J., and Cooper, H. L. Purification and composition of the human tumor-associated glycoprotein (TAG-72) defined by monoclonal antibodies CC49 and B72.3. Cancer Res., *48:* 6811–6818, 1988.
31. Nyhus, J. K., Wolford, C. C., Friece, C. R., Nelson, B., Sampsel, J. W., and Barbera-Guillem, E. IgG-recognizing shed tumor-associated antigens can promote tumor invasion and metastasis. Cancer Immunol. Immunother., *50:* 361–372, 2001.
32. Barbera-Guillem, E., May, K. F., Jr., Nyhus, J. K., and Nelson, M. B. Promotion of tumor invasion by cooperation of granulocytes and macrophages activated by antitumor antibodies. Neoplasia, *1:* 453–460, 1999.
33. Rak, J., Mitsuhashi, Y., Bayko, L., Filmus, J., Shirasawa, S., Sasazuki, T., and Kerbel, R. S. Mutant ras oncogenes up regulate VEGF/VPF expression: implications for induction and inhibition of tumor angiogenesis. Cancer Res., *55:* 4575–4580, 1995.
34. Yoshiji, H., Gomez, D. E., Shibuya, M., and Thorgeirsson, U. P. Expression of vascular endothelial growth factor, its receptor, and other angiogenic factors in human breast cancer. Cancer Res., *56:* 2013–2016, 1996.
35. Presta, L. G., Chen, H., O'Connor, S. J., Chisholm, V., Meng, Y. G., Krummen, L., Winkler, M., and Ferrara, N. Humanization of an anti-vascular endothelial growth factor monoclonal antibody for the therapy of solid tumors and other disorders. Cancer Res., *57:* 4593–4599, 1997.
36. Saleh, M., Stacker, S. A., and Wilks, A. F. Inhibition of growth of C6 glioma cells *in vivo* by expression of antisense vascular endothelial growth factor sequence. Cancer Res., *56:* 393–401, 1996.
37. Borgstrom, P., Hillan, K. J., Sriramarao, P., and Ferrara, N. Complete inhibition of angiogenesis and growth of microtumors by anti-vascular endothelial growth factor neutralizing antibody: novel concepts of angiostatic therapy from intravital videomicroscopy. Cancer Res., *56:* 4032–4039, 1996.
38. Verheul, H. M., Hoekman, K., Luykx-de Bakker, S., Eekman, C. A., Folman, C. C., Broxterman, H. J., and Pinedo, H. M. Platelet: transporter of vascular endothelial growth factor. Clin. Cancer Res., *3:* 2187–2190, 1997.
39. Wartiovaara, U., Salven, P., Mikkola, H., Lassila, R., Kaukonen, J., Joukov, V., Orpana, A., Ristimaki, A., Heikinheimo, M., Joensuu, H., Alitalo, K., and Palotie, A. Peripheral blood platelets express VEGF-C and VEGF, which are released during platelet activation. Thromb. Haemostasis, *80:* 171–175, 1998.
40. Salven, P., Orpana, A., and Joensuu, H. Leukocytes and platelets of patients with cancer contain high levels of vascular endothelial growth factor. Clin. Cancer Res., *5:* 487–491, 1999.
41. Xiong, M., Elson, G., Legarda, D., and Leibovich, S. J. Production of vascular endothelial growth factor by murine macrophages: regulation by hypoxia, lactate, and the inducible nitric oxide synthase pathway. Am. J. Pathol., *153:* 587–598, 1998.
42. Kranz, A., Mattfeldt, T., and Waltenberger, J. Molecular mediators of tumor angiogenesis: enhanced expression and activation of vascular endothelial growth factor receptor KDR in primary breast cancer. Int. J. Cancer, *84:* 293–298, 1999.
43. van Ravenswaay Claasen, H. H., Kluin, P. M., and Fleuren, G. J. Tumor infiltrating cells in human cancer. On the possible role of CD16+ macrophages in antitumor cytotoxicity. Lab. Investig., *67:* 166–174, 1992.
44. Brunda, M. J., Sulich, V., Wright, R. B., and Palleroni, A. V. Tumoricidal activity and cytokine secretion by tumor-infiltrating macrophages. Int. J. Cancer, *48:* 704–708, 1991.
45. Caruso, R. A., Vitullo, P., Modesti, A., and Inferrera, C. Small early gastric cancer with special reference to macrophage infiltration. Mod. Pathol., *12:* 386–390, 1999.
46. Lu, B., Rutledge, B. J., and Gu, L. Abnormalities in monocyte recruitment and cytokine expression in monocyte chemoattractant protein 1-deficient mice. J. Exp. Med., *187:* 601–608, 1998.
47. Hemmerlein, B., Johanns, U., Kugler, A., Reffelmann, M., and Radzun, H. J. Quantification and *in situ* localization of MCP-1 mRNA and its relation to the immune response in renal cell carcinoma. Cytokine, *13:* 227–233, 2001.
48. Ueno, T., Toi, M., Saji, H., Muta, M., Bando, H., Kuroi, K., Koike, M., Inadera, H., and Matsushima, K. Significance of macrophage chemoattractant protein-1 in macrophage recruitment, angiogenesis, and survival in human breast cancer. Clin. Cancer Res., *6:* 3282–3289, 2000.
49. Shanley, T. P., Schmal, H., Warner, R. L., Schmid, E., Friedl, H. P., and Ward, P. A. Requirement for C-X-C chemokines (macrophage inflammatory protein-2 and cytokine-induced neutrophil chemoattractant) in IgG immune complex-induced lung injury. J. Immunol., *158:* 3439–3448, 1997.
50. Dubuisson, L., Bioulac-Sage, P., Boussarie, L., Quinton, A., Saric, J., de Mascarel, A., and Balabaud, C. Removal of cellular debris formed in the Disse space in patients with cholestasis. Virchows Arch. A Pathol. Anat. Histopathol., *410:* 501–507, 1987.
51. Jeltsch, M., Kaipainen, A., Joukov, V., Meng, X., Lakso, M., Rauvala, H., Swartz, M., Fukumura, D., Jain, R. K., and Alitalo, K. Hyperplasia of lymphatic vessels in VEGF-C transgenic mice. Science (Wash. DC), *276:* 1423–1425, 1997.
52. Skobe, M., Hawighorst, T., Jackson, D. G., Prevo, R., Janes, L., Velasco, P., Riccardi, L., Alitalo, K., Claffey, K., and Detmar, M. Induction of tumor lymphangiogenesis by VEGF-C promotes breast cancer metastasis. Nat. Med., *7:* 192–198, 2001.
53. Swift, M. E., Kleinman, H. K., and DiPietro, L. A. Impaired wound repair and delayed angiogenesis in aged mice. Lab. Investig., *79:* 1479–1487, 1999.
54. Holash, J., Maisonpierre, P. C., Compton, D., Boland, P., Alexander, C. R., Zagzag, D., Yancopoulos, G. D., and Wiegand, S. J. Vessel cooption, regression, and growth in tumors mediated by angiopoietins and VEGF. Science (Wash. DC), *284:* 1994–1998, 1999.
55. Bansal, S. C., Bansal, B. R., Thomas, H. L., Siegel, P. D., Rhoads, J. E., Jr., Cooper, D. R., Terman, D. S., and Mark, R. *Ex vivo* removal of serum IgG in a patient with colon carcinoma: some biochemical, immunological and histological observations. Cancer (Phila.), *42:* 1–18, 1978.
56. Canevari, S., Pupa, S. M., and Menard, S. 1975–1995 revised anti-cancer serological response: biological significance and clinical implications. Ann. Oncol., *7:* 227–232, 1996.
57. Lee, Y. T., Sheikh, K. M., Quismorio, F. P., Jr., and Friou. G. J. Circulating anti-tumor and autoantibodies in breast carcinoma: relationship to stage and prognosis. Breast Cancer Res. Treat., *6:* 57–65, 1985.